Journal of Sound and Vibration (2002) **250**(2), 181–196
doi:10.1006/jsvi.2001.3710, available online at http://www.idealibrary.com on IDEAL®

MEASUREMENT OF THE VISCOELASTIC PROPERTIES OF DAMPING MATERIALS: ADAPTATION OF THE WAVE PROPAGATION METHOD TO TEST SAMPLES OF SHORT LENGTH

P. LEMERLE

Laboratoire de Modélisation des Systèmes Mécaniques de Prévention, INRS, Avenue de Bourgogne BP no. 27, 54501 *Vandoeuvre Cedex, France. E-mail: lemerle@inrs.fr*

(*Received* 3 *October* 2000, *and in final form* 25 *January* 2001)

Wave propagation methods allow the deduction of the viscoelastic damping properties of materials from the waveform pattern of a transitory wave: the wave profile is recorded at two travel distances in a thin bar made of the medium studied. In the case of linear viscoelasticity, the characteristics of the material are deduced directly from the transfer function of the two pulses measured. From a theoretical point of view, these methods are of great interest as they bridge a gap between vibratory methods and ultrasonic methods, allowing results to be obtained in a frequency range covering one and a half to two decades in the audiometric range (20 Hz–20 kHz). However, they have not been used much in industrial applications due to the difficulty and cost involved in producing samples in the form of bars. This study shows how this type of method can be adapted to measuring the viscoelastic properties of damping materials using reduced size and common shaped samples such as end-stop buffers.

1. INTRODUCTION

It is at the design stage that manufacturers endeavour to reduce the noise and vibration of machines. Damping and decoupling are solutions frequently adopted by engineering and design departments and users of machines on account of their efficiency and ease of application. These attenuation techniques generally make use of viscoelastic materials such as elastomers, in other words, materials with damping properties that allow part of the vibratory energy to be dissipated in the form of heat. Elastomers are used in the form of isolating supports (vibration isolators), composites (sandwich materials) or isolation coverings to dampen structural vibrations in the medium and high-frequency ranges.

The structure calculation software products available today such as *finite-element codes* allow these isolation systems to be sized. Numerical simulation of the vibratory behaviour of elastomer structures, however, requires knowledge of their intrinsic properties: Young's modulus E and the loss factor β or any other pair of equivalent viscoelastic functions including the phase velocity c and the damping coefficient α.

Different methods allow the E and β characteristics of materials to be evaluated. Three broad families can be distinguished: vibratory, ultrasonic and wave propagation methods. Vibratory methods consist either in measuring the resonance characteristics of simple structures such as beams (Oberst method [1]) and plates (SAE—Society of Automotive Engineers—method [2]) or in directly measuring the dynamic rigidity of a sample of

0022-460X/02/070181 + 16 $35.00/0

material (viscoelasticimetry [3]). These methods are limited to a few hundred Hz for materials with the highest damping properties. In contrast, ultrasonic method [4–6] allow the viscoelastic properties of materials to be determined for frequencies between 0·5 and 5 MHz. The field of application of wave propagation methods lies between these two frequency ranges. These techniques have been known since 1958 [7] and have been gradually improved during these last 40 years [8–13]. Their principle consists in measuring at two points or at two different instants the waveform of a plane wave propagating in a test item composed of a thin bar about 1 m in length. The transfer function between these two measurements then allows the viscoelastic parameters to be obtained. Wave propagation methods have the advantage of directly providing results in the audible range with a low-cost experimental set-up that does not require any specific skills. However, these methods are used little in industry as the elastomer test samples in bar form are both difficult and costly to produce. This study shows how to adapt the principle of plane wave propagation measurement to more commonly sized samples such as end-stop buffers or studs measuring only a few centimetres.

2. PRINCIPLE OF THE PROPOSED METHOD

The proposed method consists in creating a plane impact wave in a bar with accurately known viscoelastic properties and at the end of which a sample of the material to be characterized has been glued. This sample, only a few centimetres in length, is intended to disturb the propagation of the wave in the reference bar. The viscoelastic characteristics of the reference bar are known and it is sufficiently long to isolate the first passage of the wave from its successive echoes. A sensor records the progressive waves that are propagated in the bar.

By assuming that the viscoelastic parameters of the sample are known, it is possible to calculate the time history measured by the sensor by applying the propagation equations to the first wave front observed. Measuring the viscoelastic properties of the sample therefore leads to the resolution of an identification problem: the viscoelastic characteristics of the sample are deduced from an optimization procedure consisting in identifying the propagation model with the time history measured.

2.1. PROPAGATION EQUATIONS IN A THIN BAR

The length of the bar (compared to its cross-section) in such that the propagation problem can be considered as a one-dimensional problem. In these conditions, let us designate $f(x, t)$ the pulse at a distance x and at a time t. f can represent either the strain ε, or the material velocity v. The Fourier transform of $f(x, t)$ with respect to time is designated $\bar{f}(x, \omega)$. It can then be shown [14, 15] that the motion equations governing unidirectional wave propagation in the material lead to the general solution of the form

$$\bar{f}(x, \omega) = X_1 e^{-\gamma(\omega)x} + X_2 e^{\gamma(\omega)x}, \tag{1}$$

with

$$\gamma(\omega) = \alpha(\omega) + i\omega/c(\omega).$$

$X_1(\omega)$ and $X_2(\omega)$ are determined by the initial and boundary conditions, whereas the damping coefficient $\alpha(\omega)$ and the phase velocity $c(\omega)$ are intrinsic properties of the material.

Inverse Fourier transformation of equation (1) results in

$$f(x,t)=\frac{1}{2\pi}\int_{-\infty}^{+\infty}X_1(\omega)\mathrm{e}^{-\alpha(\omega)x}\mathrm{e}^{\mathrm{i}\omega[t-(x/c(\omega))]}\,\mathrm{d}\omega+\frac{1}{2\pi}\int_{-\infty}^{+\infty}X_2(\omega)\mathrm{e}^{\alpha(\omega)x}\mathrm{e}^{\mathrm{i}\omega[t+(x/c(\omega))]}\,\mathrm{d}\omega. \quad (2)$$

The two terms on the right-hand side of the equation represent waves propagating in increasing and decreasing x directions respectively.

2.2 OVERVIEW OF THE "SEPARATE PULSE" METHOD

By placing the x origin at the end of the bar submitted to impact, and by observing only the progressive wave before its first echo, propagation equation (2) then becomes

$$f(x,t)=\frac{1}{2\pi}\int_{-\infty}^{+\infty}\bar{f}(0,\omega)\mathrm{e}^{-\alpha(\omega)x+\mathrm{i}\omega[t-x/c(\omega)]}\,\mathrm{d}\omega. \quad (3)$$

Taking the inverse Fourier transform of (3) and expressing it in polar form:

$$\bar{f}(x,\omega)=\rho(x,\omega)\mathrm{e}^{\mathrm{i}\theta(x,\omega)}. \quad (4)$$

The principle of the "separate pulse" method developed by Blanc [16] consists in expressing equation (4) for two distances of travel x_1 and x_2. The resolution of the resulting system then leads to the following equations:

$$c(\omega)=-\omega\frac{x_2-x_1}{\theta(x_2,\omega)-\theta(x_1,\omega)},\qquad \alpha(\omega)=-\frac{1}{x_2-x_1}\log\left(\frac{\rho(x_2,\omega)}{\rho(x_1,\omega)}\right). \quad (5)$$

Any other viscoelastic function characteristics, for example Young's modulus and the loss factor, can be deduced from $c(\omega)$ and $\alpha(\omega)$.

The "separate pulse" method can only be applied in the case where the successive pulse echoes are not superimposed on the first wave-front, implying that the bar must be long enough in relation to the scattering of the progressive wave, and therefore with respect to the damping properties of the material. In the case of rubber, for example, the length of the bar must be about 1 m to satisfy this condition.

2.3. CHARACTERIZATION OF THE REFERENCE BAR AND OF THE ELASTOMER CONTROL BY THE "SEPARATE PULSE" METHOD

The "separate pulse" method was used to measure the viscoelastic properties of the reference bar (made of PVC: polyvinyl chloride). The same method was also used to characterize a "control" elastomer bar. This measurement was employed as the standard measurement and allowed validation of the proposed method. Two velocity sensors (audio cells) were used for each bar to measure the wave profiles simultaneously at two travel distances x_1 and x_2. The results of the measurements of both materials are given in Figure 1. In the frequency range valid for these measurements, namely < 5000 Hz for PVC and < 2000 Hz for elastomer, both materials have a constant phase velocity ($c = 1679$ m/s for PVC and $c = 151{\cdot}4$ m/s for elastomer) and a damping coefficient proportional to the frequency ($\alpha = \alpha_0 f$, with $\alpha_0 = 6{\cdot}22\times10^{-5}\,\mathrm{m}^{-1}/\mathrm{Hz}$ for PVC and $\alpha_0 = 3{\cdot}0\times10^{-3}\,\mathrm{m}^{-1}/\mathrm{Hz}$ for elastomer).

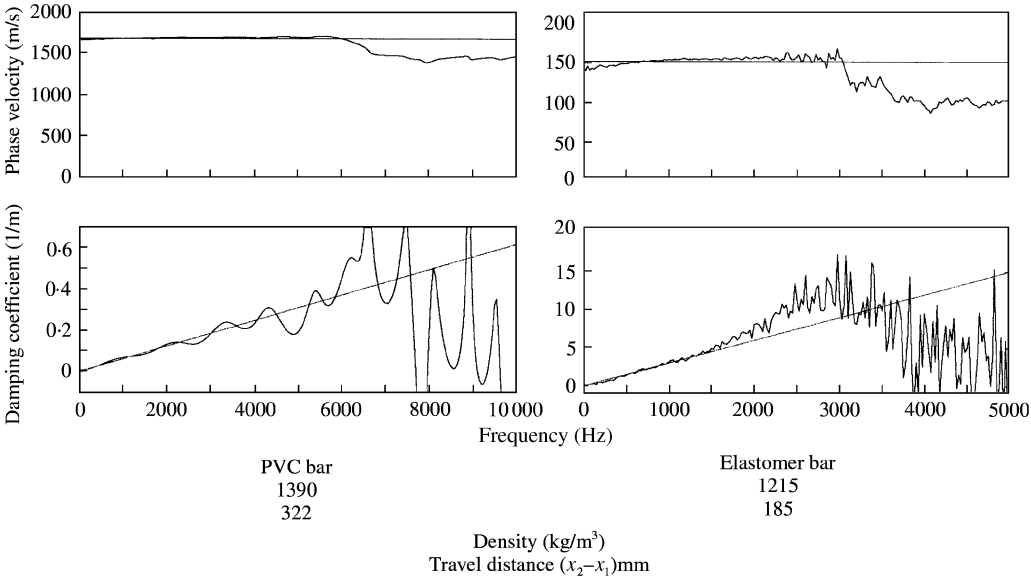

Figure 1. Measurements of the viscoelastic properties of the reference bar (PVC) and of the control material (elastomer bar).

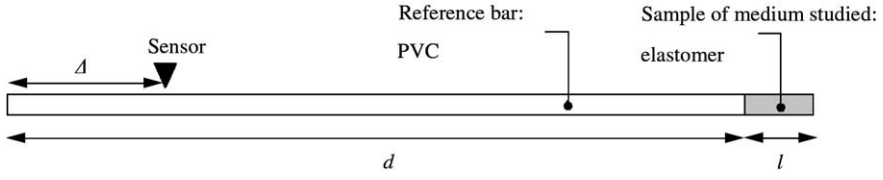

Figure 2. Compositon of a test bar.

2.4. REFLECTION AND TRANSMISSION CONDITIONS

In contrast to standard wave propagation methods such as the "separate pulse" method, the sample bar is not homogeneous in the case of the proposed method. It is composed of the reference bar (PVC bar) with a sample taken from the "control" bar (elastomer bar) glued to its end (see Figure 2). The length l of the sample was arbitrarily chosen at 45 mm.

The propagation of a plane impact wave in either material is expressed by the same equation (2). Only the coefficients $X_1(\omega)$ and $X_2(\omega)$ as well as the viscoelastic characteristics $c(\omega)$ and $\alpha(\omega)$ involved in the transport terms are different.

As previously stated, terms $X_1(\omega)$ and $X_2(\omega)$ are determined by the boundary conditions at the end of the bar as well as the reflection and transmission boundary conditions between the two media. The transmission and reflection magnitudes are deduced from the expression of the pressure and velocity continuity conditions at the interface between the two materials and which is shown schematically in Figure 3.

The velocity continuity can be expressed as

$$X_i^{1\to 2} + X_r^{1\to 2} = X_t^{1\to 2}. \tag{6}$$

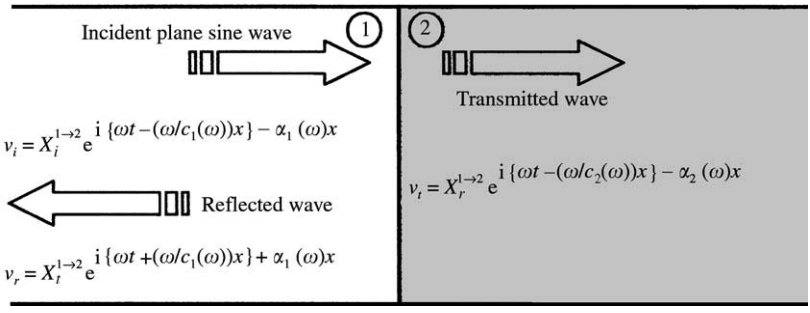

Figure 3. Transmission of velocity plane waves between the two material media.

The equation of the conservation of momentum gives the pressure and velocity dependency relationship:

$$\rho\frac{\partial v}{\partial t}+\frac{\partial p}{\partial x}=0 \Rightarrow \begin{cases} p=\rho v/(1/c(\omega)-i(\alpha(\omega)/\omega)) & \text{for an incident wave,} \\ p=-\rho v/(1/c(\omega)-i(\alpha(\omega)/\omega)) & \text{for a reflected wave,} \end{cases} \tag{7}$$

where ρ represents the density and p the pressure.

Relationships (7) allow the equation of the pressure continuity at the interface to be expressed as

$$\rho_1 X_i^{1\to2}\left(\frac{1}{c_2(\omega)}-i\frac{\alpha_2(\omega)}{\omega}\right)-\rho_1 X_r^{1\to2}\left(\frac{1}{c_2(\omega)}-i\frac{\alpha_2(\omega)}{\omega}\right)=\rho_2 X_t^{1\to2}\left(\frac{1}{c_1(\omega)}-i\frac{\alpha_1(\omega)}{\omega}\right). \tag{8}$$

The expressions of the magnitudes of the reflected and transmitted wave, respectively, $X_r^{1\to2}$ and $X_t^{1\to2}$, are deduced from equations (5) and (8)

$$X_r^{1\to2}=\frac{\rho_1(1/c_2(\omega)-i\,\alpha_2(\omega)/\omega)-\rho_2(1/c_1(\omega)-i\,\alpha_1(\omega)/\omega)}{\rho_2(1/c_1(\omega)-i\,\alpha_1(\omega)/\omega)+\rho_1(1/c_2(\omega)-i\,\alpha_2(\omega)/\omega)},$$

$$X_t^{1\to2}=\frac{2\rho_1(1/c_2(\omega)-i\,\alpha_2(\omega)/\omega)}{\rho_2(1/c_1(\omega)-i\,\alpha_1(\omega)/\omega)+\rho_1(1/c_2(\omega)-i\,\alpha_2(\omega)/\omega)}. \tag{9}$$

The same reasoning is applied in order to determine the reflection magnitude $X_r^{2\to1}$ and the transmission magnitude $X_t^{2\to1}$ for an incident wave originating in medium ②and being propagated towards medium ①:

$$X_r^{2\to1}=-X_r^{1\to2}$$

$$X_t^{2\to1}=\frac{2\rho_2(1/c_1(\omega)-i\alpha_1(\omega)/\omega)}{\rho_2(1/c_1(\omega))-i\alpha_1(\omega)/\omega+\rho_1(1/c_2(\omega)-i\alpha_2(\omega)/\omega)}. \tag{10}$$

It is verified that formula (9) also gives the total reflection conditions of the wave at the end of the bar: $X_r^{1\to2}=1$ by considering that air has a negligible density compared to PVC or elastomer ($\rho_1 \gg \rho_2$).

The time history measured by the sensor can therefore, in theory, be calculated from formula (2), ensuring that the reflection and transmission magnitudes and the associated transport terms for each passage of the progressive wave at the interface between the two materials or at the end of the bar are taken into account in the expression of $X_1(\omega)$ and $X_2(\omega)$.

Next, it is considered that, like PVC, elastomer as a constant phase velocity ($c_2(\omega) = c_2$) and that its damping coefficient is proportional to frequency ($\alpha_2(\omega) = \alpha_2\omega$). Equation (9) then becomes

$$X_r^{1\to 2} = \frac{\rho_1((1/c_2) - \mathrm{i}\alpha_2) - \rho_2((1/c_1) - \mathrm{i}\alpha_1)}{\rho_2((1/c_1) - \mathrm{i}\alpha_1) + \rho_1((1/c_2) - \mathrm{i}\alpha_2)},$$

$$X_t^{1\to 2} = \frac{2\rho_1((1/c_2) - \mathrm{i}\alpha_2)}{\rho_2((1/c_1) - \mathrm{i}\alpha_1) + \rho_1((1/c_2) - \mathrm{i}\alpha_2)}. \tag{11}$$

with c_2 and α_2 the two viscoelastic parameters sought.

2.5. MODELLING THE PROPAGATION BY SUPERPOSITION OF THE WAVE TRAINS

Let one suppose that the velocity measurement has allowed isolation of the first passage of the wave on abscissa Δ (see Figure 2), the axis origin chosen arbitrarily at this point and $\bar{f}(0, \omega)$ designated the Fourier transform of the first wave-front. The time history measured by the velocity sensor can then be calculated by applying the principle of superposition of echoes (principle derived from the hypothesis of linearity of the propagation problem), the echoes being determined from the incident wave $\bar{f}(0, \omega)$ by means of the propagation equations. The echoes multiply very quickly due to the fact that their propagation velocities are high compared to the dimensions of the bar. It is for this reason that the study was intentionally limited to the signal measured over a time interval equal to the time taken by the incident wave to travel six lengths of the bar.

In this time interval, the direct reflections of the incident wave between both ends of the reference bar are expressed by six terms (see Figure 4).

$$\begin{aligned}
&\Lambda^1 = X_r^{1\to 2}\,\bar{f}(0,\omega)\mathrm{e}^{-2(d-\Delta)(\alpha_1+(1/c_1))\omega}, && \Lambda^2 = X_r^{1\to 2}\,\bar{f}(0,\omega)\mathrm{e}^{-2d(\alpha_1+(1/c_1))\omega},\\
&\Lambda^3 = (X_r^{1\to 2})^2\bar{f}(0,\omega)\mathrm{e}^{-2(2d-\Delta)(\alpha_1+(1/c_1))\omega}, && \Lambda^4 = (X_r^{1\to 2})^2\bar{f}(0,\omega)\mathrm{e}^{-4d(\alpha_1+(1/c_1))\omega},\\
&\Lambda^5 = (X_r^{1\to 2})^3\bar{f}(0,\omega)\mathrm{e}^{-2(3d-\Delta)(\alpha_1+(1/c_1))\omega}, && \Lambda^6 = (X_r^{1\to 2})^3\bar{f}(0,\omega)\mathrm{e}^{-6d(\alpha_1+(1/c_1))\omega}.
\end{aligned} \tag{12}$$

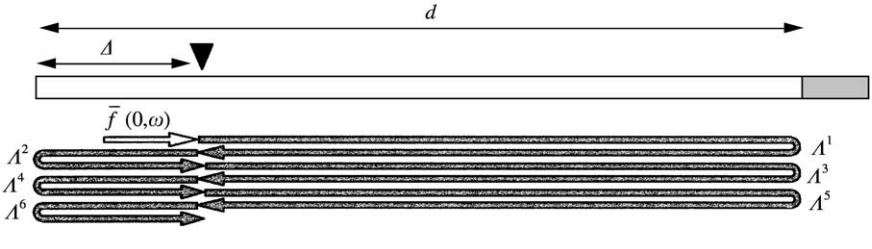

Figure 4. Direct reflections in the reference bar.

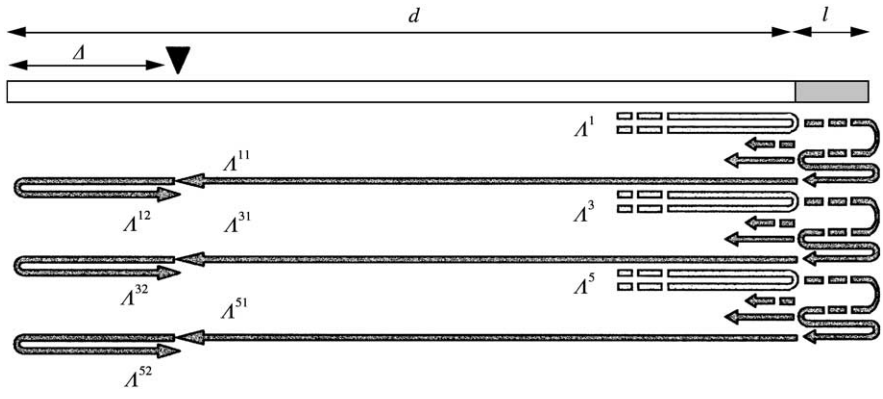

Figure 5. First crossing of the elastomer sample.

A wave transmitted in the elastomer sample is associated with each of the echoes Δ^1, Δ^3 and Δ^5. This wave travels the length of the sample, is reflected at its free end back to the interface and again generates a wave in the PVC bar and an echo in the sample. This pattern is reproduced indefinitely until attenuation of the progressive wave in the sample, resulting in the creation of a distinct wave train that propagates in the PVC bar. In practice, only the first n reflections inside the sample are taken into account, as the subsequent reflections occur outside the time interval of the study. In the case of the elastomer studied, n was chosen as equal to 5 and it was subsequently verified that this value allowed all the reflections in the time interval studied to be taken into account. Figure 5 illustrates the first crossing of an elastomer sample.

$$\Delta^{11} = \sum_{k=1}^{n} (X_t^{2\to1}(X_r^{2\to1})^{k-1} \mathrm{e}^{-2kl(\alpha_2+(1/c_2))\omega}) \bar{f}(0,\omega) \mathrm{e}^{-2(d-\Delta)(\alpha_1+(1/c_1))\omega},$$

$$\Delta^{12} = \sum_{k=1}^{n} (X_t^{2\to1}(X_r^{2\to1})^{k-1} \mathrm{e}^{-2kl(\alpha_2+(1/c_2))\omega}) \bar{f}(0,\omega) \mathrm{e}^{-2d(\alpha_1+(1/c_1))\omega},$$

$$\Delta^{31} = \sum_{k=1}^{n} (X_t^{2\to1}(X_r^{2\to1})^{k-1} \mathrm{e}^{-2kl(\alpha_2+(1/c_2))\omega})(X_r^{1\to2}) \bar{f}(0,\omega) \mathrm{e}^{-2(2d-\Delta)(\alpha_1+(1/c_1))\omega},$$

$$\Delta^{32} = \sum_{k=1}^{n} (X_t^{2\to1}(X_r^{2\to1})^{k-1} \mathrm{e}^{-2kl(\alpha_2+(1/c_2))\omega})(X_r^{1\to2}) \bar{f}(0,\omega) \mathrm{e}^{-4d(\alpha_1+(1/c_1))\omega},$$

$$\Delta^{51} = \sum_{k=1}^{n} (X_t^{2\to1}(X_r^{2\to1})^{k-1} \mathrm{e}^{-2kl(\alpha_2+(1/c_2))\omega})(X_r^{1\to2})^2 \bar{f}(0,\omega) \mathrm{e}^{-2(3d-\Delta)(\alpha_1+(1/c_1))\omega},$$

$$\Delta^{52} = \sum_{k=1}^{n} (X_t^{2\to1}(X_r^{2\to1})^{k-1} \mathrm{e}^{-2kl(\alpha_2+(1/c_2))\omega})(X_r^{1\to2})^2 \bar{f}(0,\omega) \mathrm{e}^{-6d(\alpha_1+(1/c_1))\omega}. \quad (13)$$

The wave-trains resulting from the passage through the sample are propagated in the PVC bar and reflected at its ends. Among these terms of successive reflections, only those with

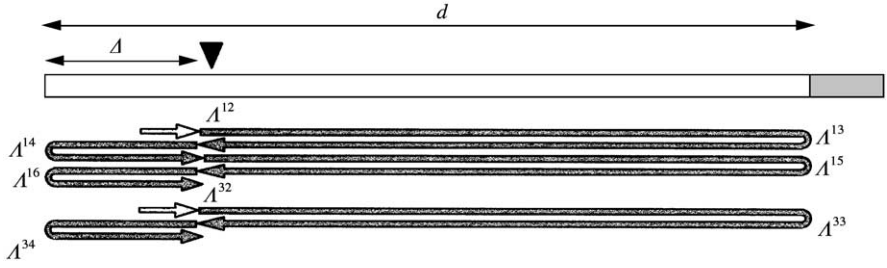

Figure 6. Reflections of the first crossing of the elastomer sample.

a distance of travel of less than six lengths of the bar are retained. Reflections of the first crossing of the elastomer sample is shown in Figure 6.

$$\Lambda^{13} = \Lambda^{12} X_r^{1\to 2} e^{-2(d-\Delta)(\alpha_1 + 1/c_1)\omega}, \qquad \Lambda^{14} = \Lambda^{12} X_r^{1\to 2} e^{-2d(\alpha_1 + 1/c_1)\omega},$$

$$\Lambda^{15} = \Lambda^{12} (X_r^{1\to 2})^2 e^{-2(2d-\Delta)(\alpha_1 + 1/c_1)\omega}, \qquad \Lambda^{16} = \Lambda^{12} (X_r^{1\to 2})^2 e^{-4d(\alpha_1 + 1/c_1)\omega},$$

$$\Lambda^{33} = \Lambda^{32} X_r^{1\to 2} e^{-2(d-\Delta)(\alpha_1 + 1/c_1)\omega}, \qquad \Lambda^{34} = \Lambda^{32} X_r^{1\to 2} e^{-2d(\alpha_1 + 1/c_1)\omega}. \tag{14}$$

A wave-train transmitted in the elastomer sample is also associated with each of these reflections (Λ^{13}, Λ^{15} and Λ^{33}). As per the process of multiple reflections previously described (see Figure 5), a new wave-train is transmitted in the PVC bar:

$$\Lambda^{131} = \Lambda^{12} \sum_{k=1}^{n} (X_t^{2\to 1} (X_r^{2\to 1})^{k-1} e^{-2kl(\alpha_2 + 1/c_2)\omega}) e^{-2(d-\Delta)(\alpha_1 + 1/c_1)\omega},$$

$$\Lambda^{132} = \Lambda^{12} \sum_{k=1}^{n} (X_t^{2\to 1} (X_r^{2\to 1})^{k-1} e^{-2kl(\alpha_2 + 1/c_2)\omega}) e^{-2d(\alpha_1 + 1/c_1)\omega},$$

$$\Lambda^{151} = \Lambda^{14} \sum_{k=1}^{n} (X_t^{2\to 1} (X_r^{2\to 1})^{k-1} e^{-2kl(\alpha_2 + 1/c_2)\omega}) e^{-2(d-\Delta)(\alpha_1 + 1/c_1)\omega},$$

$$\Lambda^{152} = \Lambda^{14} \sum_{k=1}^{n} (X_t^{2\to 1} (X_r^{2\to 1})^{k-1} e^{-2kl(\alpha_2 + 1/c_2)\omega}) e^{-2d(\alpha_1 + 1/c_1)\omega},$$

$$\Lambda^{331} = \Lambda^{32} \sum_{k=1}^{n} (X_t^{2\to 1} (X_r^{2\to 1})^{k-1} e^{-2kl(\alpha_2 + 1/c_2)\omega}) e^{-2(d-\Delta)(\alpha_1 + 1/c_1)\omega},$$

$$\Lambda^{332} = \Lambda^{32} \sum_{k=1}^{n} (X_t^{2\to 1} (X_r^{2\to 1})^{k-1} e^{-2kl(\alpha_2 + 1/c_2)\omega}) e^{-2d(\alpha_1 + 1/c_1)\omega}. \tag{15}$$

The second crossing occurring in the elastomer sample are portrayed in Figure 7. These wave-trains are again reflected at the end of the PVC bar as illustrated in Figure 8.

$$\Lambda^{133} = \Lambda^{132} X_r^{2\to 1} e^{-2(d-\Delta)(\alpha_1 + 1/c_1)\omega}, \qquad \Lambda^{134} = \Lambda^{132} X_r^{2\to 1} e^{-2d(\alpha_1 + 1/c_1)\omega}. \tag{16}$$

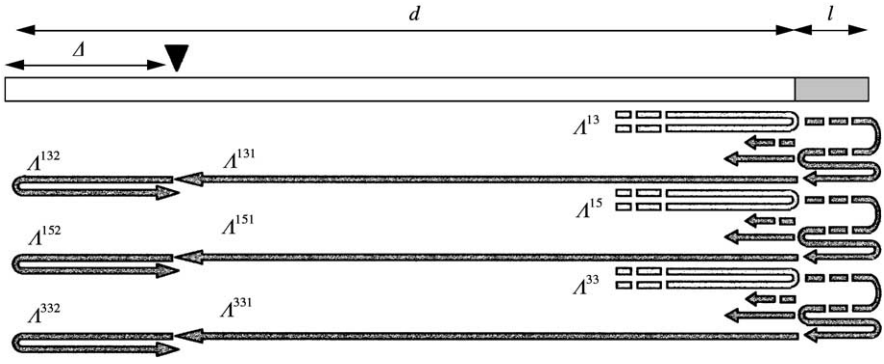

Figure 7. Second crossing of the elastomer sample.

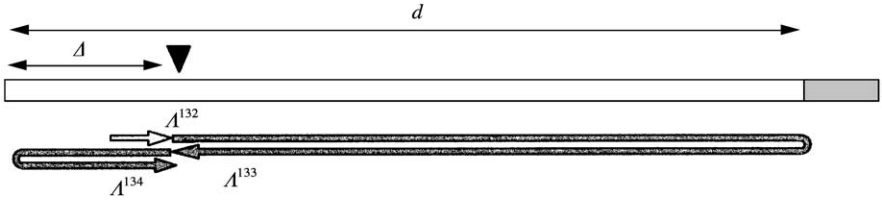

Figure 8. Reflections of the second crossing of the elastomer sample.

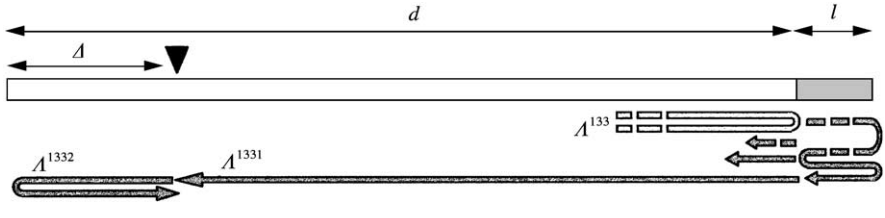

Figure 9. Third crossing of the elastomer sample.

Finally, part of these wave-trains is transmitted to the studied medium and returns to the PVC bar, as represented in Figure 9.

$$\Lambda^{1331} = \Lambda^{132} \sum_{k=1}^{n} (X_t^{2\to1})(X_r^{2\to1})^{k-1} \mathrm{e}^{-2kl(\alpha_2 + 1/c_2)\omega}) \mathrm{e}^{-2(d-\Delta)(\alpha_1 + 1/c_1)\omega},$$

$$\Lambda^{1332} = \Lambda^{132} \sum_{k=1}^{n} (X_t^{2\to1})(X_r^{2\to1})^{k-1} \mathrm{e}^{-2kl(\alpha_2 + 1/c_2)\omega}) \mathrm{e}^{-2d(\alpha_1 + 1/c_1)\omega}. \tag{17}$$

2.6. IDENTIFICATION OF THE MEASURED SIGNAL

For a given pair of values (c_2, α_2), it is therefore possible to calculate, for a limited period of time, the velocity signal which would be measured for a sample of material with these viscoelastic characteristics. By defining the measured velocity as $f(t, c_2, \alpha_2)$ and the

calculated velocity as $F(t, c_2, \alpha_2)$ and using the principle of superposition, $F(t, c_2, \alpha_2)$ can be stated according to the propagation terms previously expressed as

$$F(t, c_2, \alpha_2) = \frac{1}{2\pi}\int_{-\infty}^{+\infty} (\bar{f}(0, \omega) + \Lambda^1 + \Lambda^2 + \Lambda^3 + \Lambda^4 + \Lambda^5 + \Lambda^6)\,\mathrm{d}\omega$$

$$+ \frac{1}{2\pi}\int_{-\infty}^{+\infty} (\Lambda^{11} + \Lambda^{12} + \Lambda^{31} + \Lambda^{32} + \Lambda^{51} + \Lambda^{52} + \Lambda^{13} + \Lambda^{14} + \Lambda^{15} + \Lambda^{16}$$

$$+ \Lambda^{33} + \Lambda^{34})\,\mathrm{d}\omega$$

$$+ \frac{1}{2\pi}\int_{-\infty}^{+\infty} (\Lambda^{131} + \Lambda^{132} + \Lambda^{151} + \Lambda^{152} + \Lambda^{331} + \Lambda^{332} + \Lambda^{133} + \Lambda^{134}$$

$$+ \Lambda^{1331} + \Lambda^{1332})\,\mathrm{d}\omega. \tag{18}$$

The measurement principle proposed therefore consists in optimizing (c_2, α_2) to minimize the difference between the measured signal and the calculated signal over the time interval in question. The error between the measurement and the calculation of the velocity can be expressed as the quadratic distance between the two functions f and F:

$$\varepsilon(c_2, \alpha_2) = \sqrt{\sum_{kt_e=0}^{t_0} [f(kt_e, c_2, \alpha_2) - F(kt_e, c_2, \alpha_2)]^2}, \tag{19}$$

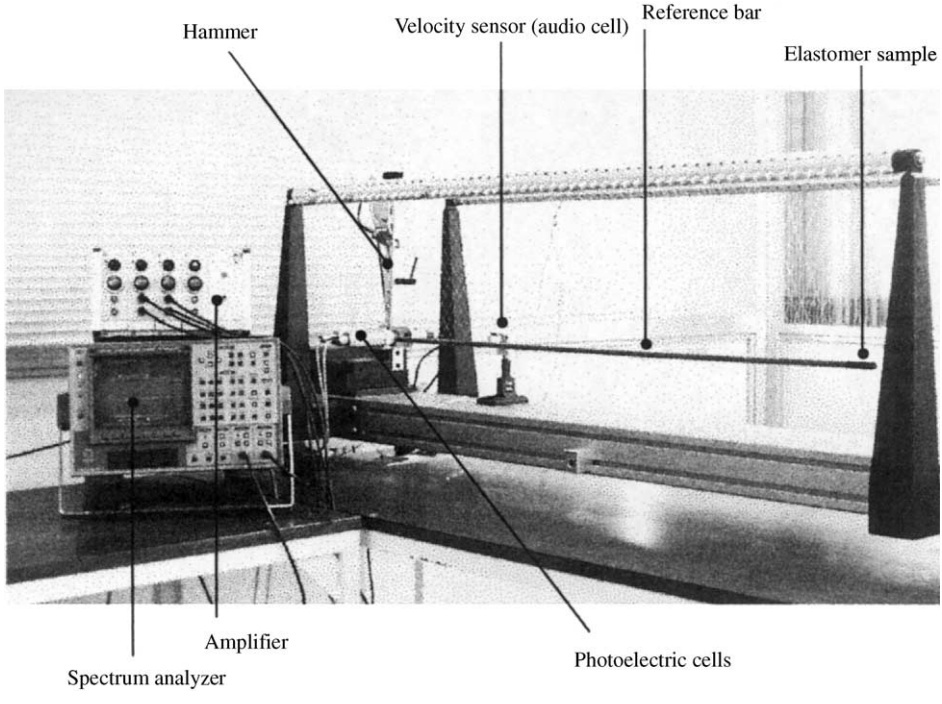

Figure 10. Overall view of the measurement system.

where t_e is the time step corresponding to the measurement sampling frequency, and t_0 represents the upper limit of the time interval being studied.

To minimize the cost function $\varepsilon(c_2, \alpha_2)$, a pre-programmed routine of the MATLAB scientific calculation software was used, namely the *fminunc* routine which employs the BFGS quasi-Newton method (Broyden–Fletcher–Goldfarb–Shanno [17–20]).

To avoid convergence problems linked to significant variations in the optimization variables, in particular those of α_2, one opted to optimize the logarithms of c_2 and α_2.

3. EXPERIMENTAL SET-UP

Figure 10 shows an overall view of the experimental set-up. The test bar is suspended by means of thin wires to give it boundary conditions close to those of a free system. The impact was produced by means of a hammer blow at the free end of the PVC bar. Photoelectric cells were fitted at this location to detect the passage of the hammer and thus trigger velocity signal acquisition. The velocity signal from the audio cell was amplified by conditioners and sent to the spectrum analyzer used as an acquisition system to digitize the velocity time history. The digitized signal was then transferred to a computer to be processed in accordance with the previously described method.

4. RESULTS AND DISCUSSION

The dimensions of the test bar, the position of the velocity sensor and the viscoelastic properties of the PVC are $l = 45$ mm, $\rho_1 = 1390$ kg/m^3, $v_1 = 1679$ m/s, $d = 974$ mm, $\rho_2 = 1215$ kg/m^3, $\alpha_1 = 6{\cdot}22 \times 10^{-5}$ m^{-1}/Hz, $\Delta = 50$ mm. The velocity time history measured by the audio cell is shown in Figure 11. To highlight the disturbance caused to the propagation of the impact wave by the presence of the elastomer, the propagation of this incident wave in a homogeneous PVC bar of length d with two free ends was also simulated.

The study period, previously defined as the time taken by the incident wave to travel six bar lengths, is that situated outside the grey zone of Figure 11.

Note: The wave velocity is proportional to the voltage delivered by the audio cell. It was therefore equivalent to deal with the velocity or directly with the audio cell output signal. The curves show the signal delivered by the audio cell, expressed in V.

Figure 12 shows the comparison of the velocity measurement and the calculation after optimization of c_2 and α_2. The optimization calculation gave the values $c_2 = 146{\cdot}9$ m/s,

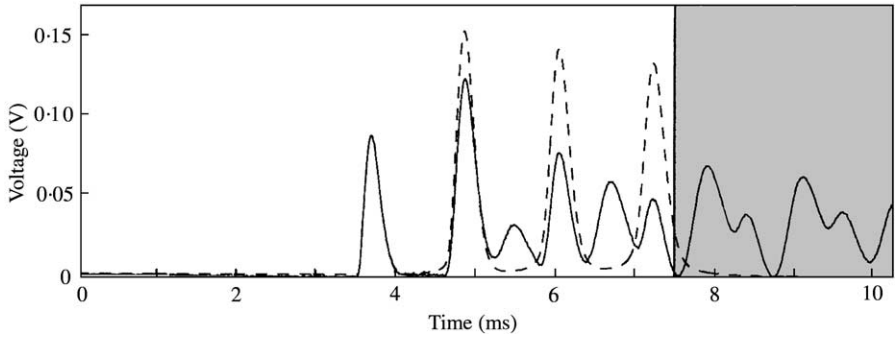

Figure 11. Influence of the elastomer sample on propagation in the test bar: ——, PVC + elastomer (measurement); – – – –, PVC alone (calculation).

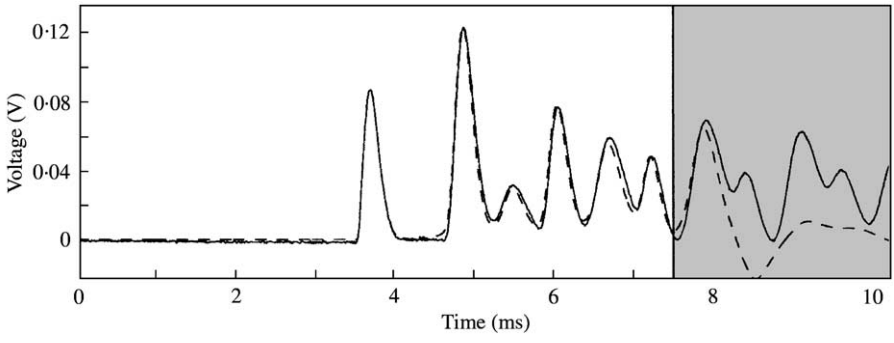

Figure 12. Identification of the propagation: ——, measurement; – – – –, identification (calculation).

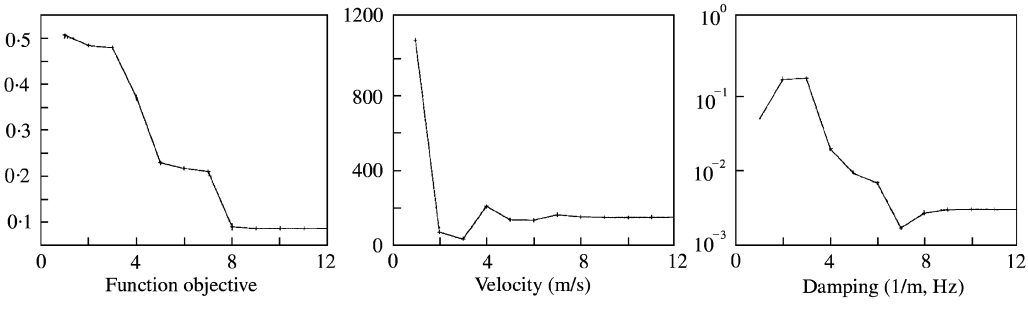

Figure 13. Convergence history.

$\alpha_2 = 2{\cdot}97 \times 10^{-3}\ \mathrm{m}^{-1}/\mathrm{Hz}$, i.e., less than 3% error in relation to the values found by the "separate pulse" method.

Figure 13 shows the convergence history. It was observed that the solution was attained quickly, taking only 12 iterations. All the echoes taken into account in the calculation of the velocity signal are shown in Figure 14. The part relative to each echo in the overall signal measured can therefore be estimated. Depending on the position of the audio cell on the bar, certain of these echoes, on account of the numerous superpositions, can either be visible or hidden. For example, the third pulse detected (in interval [5 ms, 6 ms], Figure 12) is in fact the superposition of echoes Λ^{11} and Λ^{12} (Λ^{12} being the reflection of Λ^{11} at the free end of the PVC bar). These two echoes correspond to the waves coming from the first crossing of the elastomer sample (see Figure 5) and their shape is directly linked to the viscoelastic properties of the elastomer.

It is commonly assumed that for propagation methods, an upper limit of useful frequencies can be estimated from the requirement of the one-dimensional model, saying that the wavelength must be at least 10 times the diameter of the bar specimen [21]. This condition implies, for the bar specimen tested, wavenumbers below 63 m^{-1} and frequencies below 1500 Hz.

4.1. INFLUENCE OF THE POSITION OF THE AUDIO CELL

It was verified that the values of the viscoelastic parameters obtained by optimization did not depend on the position of the audio cell on the test bar. Measurements were taken after successively positioning the cell at distances of $\Delta = 50$, 150, 250, 350 mm. Figure 15 compares the velocity measurement and its identification for each location.

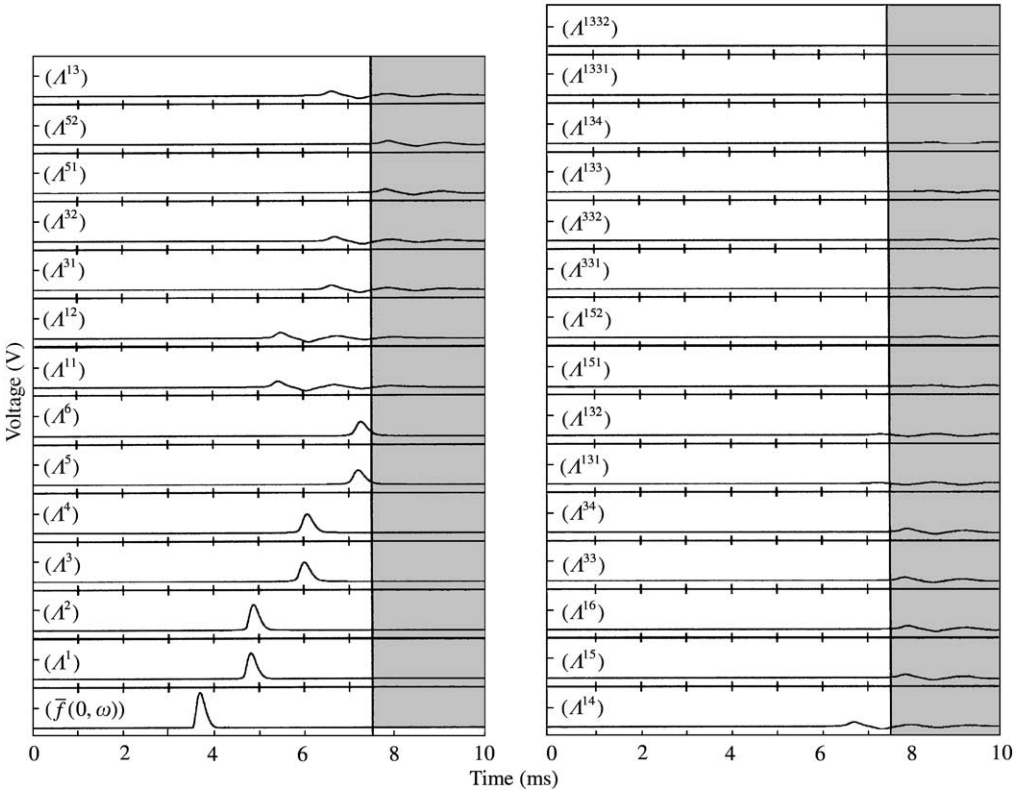

Figure 14. Shape of the echoes.

The pairs of viscoelastic parameters calculated for each cell position and corresponding to each identification shown in Figure 15 are listed in Table 1. A low dispersion of the results can be noted, thereby demonstrating that the method is reliable.

4.2. INFLUENCE OF THE LENGTH OF THE SAMPLE

It was also verified that the values of the viscoelastic parameters obtained by optimization do not depend on the length of the sample. The same measurements were therefore carried out with a shorter elastomer control (22 mm instead of 45 mm), with the results as shown in Figure 16 and Table 2.

5. CONCLUSION

This study has shown as to how it is possible to adapt pulse propagation methods to measure the viscoelastic properties of damping materials in the case of smaller-sized samples.

The method proposed allows an accurate determination of the mean value of the phase velocity and the mean slope of the damping in relation to frequency. Likewise, it is also possible to further refine the frequency-dependent models of viscoelastic parameters by, for

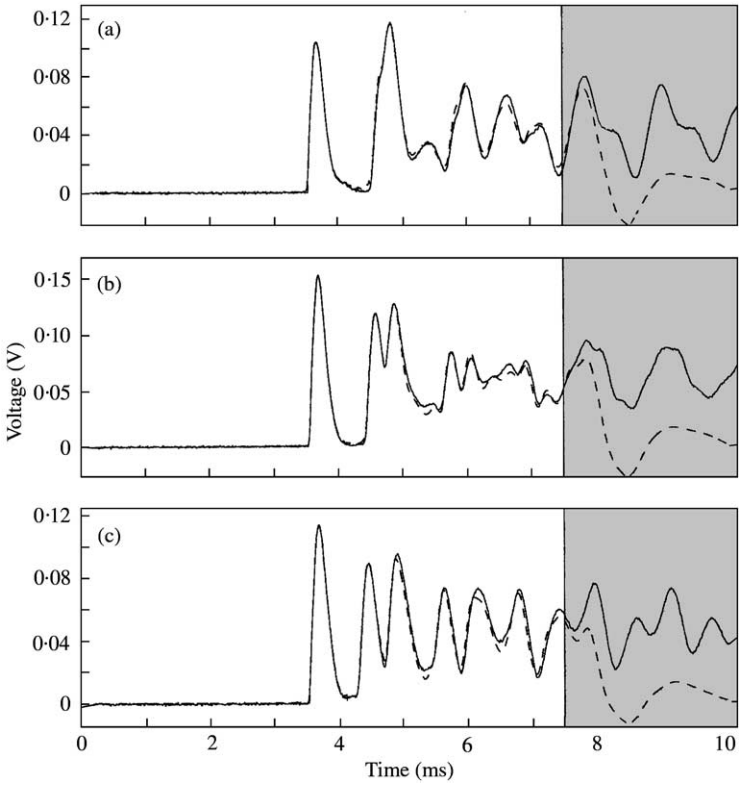

Figure 15. Influence of the position of the audio cell: ——, measurement; – – – –, identification (calculation) for Δ values (a) 150 mm; (b) 250 mm and (c) 350 mm.

TABLE 1

Results for the 45 mm elastomer sample

Position of the audio cell Δ (mm)	Phase velocity c_2 (m/s)	Damping α_2 (m^{-1}/Hz)
50	146·9	$2{\cdot}97 \times 10^{-3}$
150	147·3	$2{\cdot}36 \times 10^{-3}$
250	147·7	$2{\cdot}88 \times 10^{-3}$
350	149·9	$2{\cdot}81 \times 10^{-3}$

TABLE 2

Results for the 22 mm elastomer sample

Position of the audio cell Δ (mm)	Phase velocity c_2 (m/s)	Damping α_2 (m^{-1}/Hz)
50	143·5	$3{\cdot}28 \times 10^{-3}$
150	145·2	$2{\cdot}74 \times 10^{-3}$
250	142·68	$3{\cdot}97 \times 10^{-3}$
350	142·15	$3{\cdot}4 \times 10^{-3}$

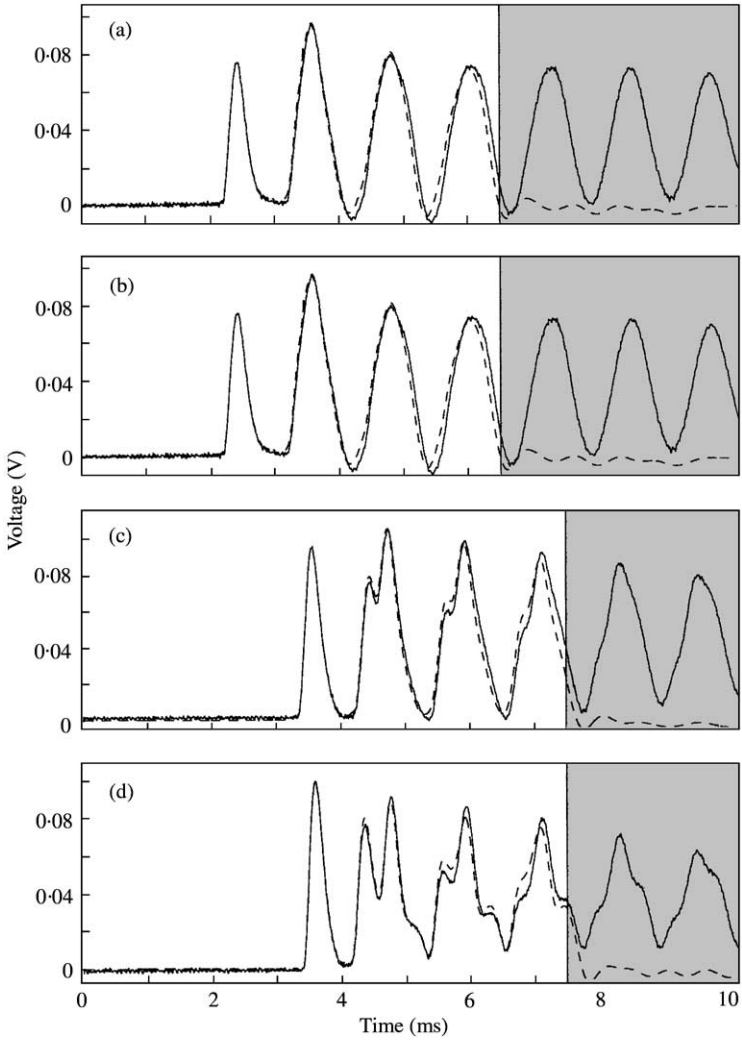

Figure 16. Influence of the length of the sample: key as per Figure 15 with Δ values of (a) 50 mm; (b) 150 mm; (c) 250 mm and (d) 350 mm.

example, employing polynomial or piecewise linear laws. In practical terms, the advantage of this method is that it allows the measurement of the viscoelastic properties of materials using common-shaped samples such as end-stop buffers or studs, which is not possible with standard pulse propagation method. It could therefore be expected that this type of an approach would be of greater interest to designers of machines and design departments.

REFERENCES

1. E. 756-83 STANDARD 1983 *Standard Method for Measuring Vibration-damping Properties of Materials*. Current edition approved July 29, 1983, published October 1983. Originally published as E 756-80. Last previous edition E 756-80.
2. T. LEWIS, P. JACKSON and O. NWANKWO 1999 *SAE Paper No*. 1999-01-1675. Design and implementation of a damping material measurement/design system.

3. B. DUPERRRAY, D. LEFEVRE and J. PEREZ 1981 *Journée AFICEP*: *Rhéologie et mise en Œuvre des Caoutchoucs*, Paris, 22 Octobre. Mesures des caractéristiques dynamiques des pâtes, polymères fondus ou élastomères non vulcanisés à l'aide du viscoélasticimètre.
4. M. DESCHAMPS 1985 *Thèse* 3ème *cycle de l'Université de Bordeaux I*. Etude en ondes planes et faisceaux bornés de la réfraction à une interface liquide-solide, application à la caractérisation viscoélastique des composites.
5. S. BAUDOIN and B. HOSTEN 1996 *Ultrasonics* **34**, 379–382. Immersion ultrasonic method to measure elastic constants and anisotropic attenuation in polymer-matrix and fibers reinforced composite materials.
6. S. JOURDAIN-BAUDOIN 1996 *Thèse* 3^{e} *cycle de l'Université Bordeaux I*. Measure et modélisation de l'atténuation ultrasonore anisotrope dans les matériaux composites.
7. S. R. BODNER and H. KOLSKY 1958 in *Proceedings of the third U. S. National Congress of Applied Mechanics*, *Providence*, *Rhode Island*, (R. M. HAYTHORNTHWAITE, editor) 495–501. Stress wave propagation in lead. New-York: ASME.
8. R. H. BLANC and F. P. CHAMPOMMIER 1976 *Journal of Sound and Vibration* **49**, 37–44. A wave-front method for determining the dynamic properties of high damping materials.
9. H. KOLSKY and S. S. LEE 1962 *Technical Report No*. 5, *Brown University*, *Providence RI*. Contract Nonr 562(30), Office of Naval Research, Washington, DC. The propagation and reflection of stress pulses in linear viscoelastic media.
10. P. S. THEOCARIS and N. PAPADOPOULOU 1978 *Polymer* **19**, 215–219. Propagation of stress waves in viscoelastic media.
11. R. M. CHRISTENSEN 1982 *Theory of Viscoelasticity*. *An Introduction*. New York: Academic Press.
12. R. H. BLANC 1971 *Doctoral Thesis*, *Université d'Aix-Marseille*, *Faculté des Sciences*, *Marseille*. Détermination de l'équation de comportement des corps viscoélastiques linéaires par une méthode d'impulsion.
13. Y. SOGABE, K. KISHIDA and K. NAKAGAWA 1982 *Bulletin of J.S.M.E.* **25**, 321–327. Wave propagation analysis for determining the dynamic properties of high damping alloys.
14. S. C. HUNTER 1960 in Progress in Solid Mechanics (I. N. SNEDDON and R. HILL, editors), Vol. 1, 1–57. Amsterdam: North-Holland; Chapter 1. Viscoelastic waves.
15. R. H. BLANC 1987 *Stage ENSTA/DYMAT M*10: *Comportements mécaniques des matériaux aux grandes vitesses de déformation*, Septermber. Fonctions rhéologiques. Viscoélasticité linéaire et ondes transitoires.
16. R. H. BLANC 1971 *Thèse de doctorat d'Etat en Mathématiques*, *Faculté des Sciences de Marseille*. Détermination de l'équation de comportement des corps viscoélastiques linéaires par une méthode d'impulsion.
17. C. G. BROYDEN 1970 *Journal of the Institute of Mathematics and its Applications* **6**, 76–90. The convergence of a class of double-rank minimization algorithms.
18. R. FLETCHER 1970 *Computer Journal*, **13**, 317–322. A new approach to variable metric algorithms.
19. D. GOLDFARB 1970 *Mathematics of Computing* **24**, 23–26. A family of variable metric updates derived by variational means.
20. D. F. SHANNO 1970 *Mathematics of Computing* **24**, 647–656. Conditioning of quasi-Newton methods for function minimization.
21. L. HILLSTRÖM, M. MOSSBERG and B. LUNDBERG 2000 *Journal of Sound and Vibration* **230**, 689–707. Identification of complex modulus from measured strains on an axially impacted bar using least squares.